

## EFFECT OF SWIFT HEAVY ION IRRADIATION ON OPTICAL AND STRUCTURAL PROPERTIES OF AMORPHOUS *Ge-As-Se* THIN FILMS

RASHMI CHAUHAN<sup>a,d\*</sup>, ARVIND TRIPATHI<sup>b</sup>, AMIT KUMAR SRIVASTAVA<sup>c</sup>, KRISHNA KANT SRIVASTAVA<sup>d</sup>

<sup>a</sup>*Department of Physic, DAV College, CSJM University, Kanpur (UP), India - 208001*

<sup>b</sup>*RFET, Datia (MP), India - 475661*

<sup>c</sup>*Material Science Programme, IIT Kanpur (UP), India - 208016*

<sup>d</sup>*Department of Physics, DBS College, CSJM University, Kanpur (UP), India - 208006*

The present study reports about changes in optical parameters of amorphous  $Ge_{7.533}As_{38.698}Se_{53.769}$  thin films upon 100 MeV Ag swift-heavy ions (SHI) for five different fluences ( $3 \times 10^{10}$ ,  $1 \times 10^{11}$ ,  $3 \times 10^{11}$ ,  $1 \times 10^{12}$ , and  $3 \times 10^{12}$  ions/cm<sup>2</sup>). Linear optical absorption coefficient ( $\alpha$ ), optical bandgap ( $E_g$ ), and linear refractive index ( $n_0$ ) of films are calculated from optical transmission spectra, and nonlinear refractive index ( $n_2$ ) is determined using semi-empirical relations. It is observed that SHI irradiation up to fluence  $3 \times 10^{12}$  ions/cm<sup>2</sup> causes reduction in optical bandgap (1.74 eV to 1.58 eV), whereas increase in linear refractive index (2.86 to 2.95) and nonlinear refractive index ( $1.37 \times 10^{-10}$  [esu] to  $2.02 \times 10^{-10}$  [esu]). These optical changes are explained in terms of structural changes using Raman spectroscopy, which predicts that swift-heavy ion irradiation causes local structural disorder, whereas optical elasticity is maintained up to threshold limit ( $3 \times 10^{12}$  ions/cm<sup>2</sup>). The utilization of the study is discussed in terms of upcoming optical technologies.

(Received January 7, 2013; Accepted February 14, 2013)

**Keywords:** Swift Heavy Ion Irradiation; Optical properties of Thin Films; Amorphous Chalcogenide; Semi-empirical relations; Raman Spectroscopy

### 1. Introduction

Chalcogenide glasses are amorphous compositions derived from key chalcogen elements i.e. S, Se, Te. The glassy derivatives of chalcogens are rich in valuable features such as photo/ion-sensitivity, large optical nonlinearity, IR transparency and low-phonon energy [1]. Periodical research updates imply intense use of these materials in upcoming optical technologies such as all-optical-signal-processing due to precise values of such characteristics, which allow fabrication of optical components functioning at low powers with improved performance [2]. Photo/ion exposure in optics/photonics is a familiar method majorly used either as a treatment tool to tailor/tune optical properties of amorphous materials [3, 4], or as a fabrication tool to compose micro/nano structures [5], depending upon the need of an application. Ion irradiation as a treatment/fabrication tool is either based on low-energy ions, where nuclear energy loss is responsible for changes in properties of the targeted material, or high-energy ions, where electronic energy loss contributes majorly. Change in properties of the targeted material depends on mass, energy and fluence of incident ions. High-energy heavy ions, also known as swift-heavy ions (SHI), have energy ranging from few ten of MeV to few GeV. Limited research groups at international level used swift-heavy ion irradiation to fabricate optical/photonic components (such as optical waveguides, and photonic

\*Corresponding author: chauhanrasmi@gmail.com

crystals) on amorphous chalcogenide. The findings as reported by some well-recognized research groups, such as Feng Qiu et al. [5] and CUDOS [6] are important from the application point of view. These studies report highly optimized performance values in amorphous chalcogenide for crucial optical parameters such as reduced optical losses (minimized to 2/2.2 dB/cm<sup>2</sup>) [5], whereas, these parameters have scope of further optimization with the help of treatment techniques such as photo/ion exposure.

Amorphous *Ge-As-Se* system provides a wide range of glass formation region; hence, a large range of compositions is available according to desired application with diversities in optical properties [7]. Optical nonlinearity in this glassy system is specifically important, which is 100 to 1000 times more than *Si* based glasses, and thus, optical components based on these materials have significant advantage of performance improvement [8]. In addition, the real advantage of these components will appear in the next generation optical systems, where conversion of optical signals into electronic signals will be eliminated by replacing optoelectronic components with optical/photonic components using a nonlinear optical material to control the light by light. In such systems, optoelectronic conversion, which causes a bottleneck in data transmission, is removed and thus processing of data, along with the rate of transmission will be as high as 1.28 Tbit/second [2].

The compositions within amorphous *Ge-As-Se* system are categorized in three phases using glass-network connectivity, which is defined in terms of mean coordination number (MCN), where MCN is the sum of product of coordination number and atomic percentages of constituent elements. These phases are flexible-floppy phase, unstressed-rigid phase (intermediate phase) and stressed-rigid phase [9-12]. Among these phases intermediate phase (IP) is a novel, optically elastic and self-organized phase ( $2.4 < \text{MCN} < 2.67$ ), which is important from application point of view due to its non-aging behaviour [12, 13]. CUDOS, a well-known research group in chalcogenide photonics from Australia, reported that amorphous  $\text{Ge}_x\text{As}_y\text{Se}_{(100-x-y)}$  ( $0 < x < 40$  and  $12 < y < 40$  compositions having  $\text{MCN} \approx 2.4-2.5$ ) possess finest attributes required in the fabrication of all-optical devices [14]. These attributes include low linear losses (absorption losses  $< 0.1$  db/cm at telecommunication wavelength 1500 nm, and negligible two-photon absorption), high third-order nonlinearity ( $\approx 350$  times of *Si*), and highest possible glass transition temperature ( $\approx 250^\circ\text{C}$ ). Bulla *et al.* also observed that amorphous  $\text{Ge}_x\text{As}_y\text{Se}_{(100-x-y)}$  compositions having MCN values close to 2.45 are thermally stable [13]. G. Yang *et al.* investigated a photo-stable composition within  $\text{Ge}_x\text{As}_{45-x}\text{Se}_{55}$  chalcogenide glassy system at  $x = 10$  ( $\text{MCN} = 2.55$ ), and proposed the glassy system for high power beam delivery [2, 15]. Thus, MCN range 2.4 to 2.55 is an important region in *Ge-As-Se* glasses for fabrication of optical/photonic component using photo/ion exposure.

Present study reports about change in optical bandgap ( $E_g$ ), linear refractive index ( $n_0$ ), nonlinear refractive index ( $n_2$ ) and structural properties for intermediate phase composition amorphous  $\text{Ge}_{7.533}\text{As}_{38.698}\text{Se}_{53.769}$  ( $\text{MCN} = 2.54$ ) thin films upon 100 MeV Ag ion irradiation. Extension of present study is useful for fabrication of optical components with low-optical losses and ultra-fast optical response time.

## 2. Experimental

Bulk  $\text{Ge}_{10}\text{As}_{40}\text{Se}_{50}$  glasses were prepared by conventional melt quenching technique. For that purpose, all three corresponding elements (purity of *As*, *Se*, *Ge* 99.999%) were weighted according to their atomic percentages, and then sealed in quartz ampoules at base pressure of  $10^{-5}$  Torr. These sealed ampoules were kept inside a furnace, and heated up to  $940^\circ\text{C}$  at the rate of  $3-4^\circ\text{C}/\text{min}$  to prepare the melt. To achieve a homogeneous melt, these ampoules were frequently rocked for 10 hours at  $940^\circ\text{C}$ , and then quenched in ice water. Thermal evaporation technique was used to prepare amorphous thin films of glassy alloys onto cleaned glass substrates at room temperature inside a coating system (HIND-HIVAC Model 12A 4DT) at a base pressure of about  $10^{-6}$  Torr. 100 MeV swift heavy Ag ion irradiation was performed using a 15 UD pelletron tandem accelerator at IUAC, New Delhi for five different fluences ( $3 \times 10^{10}$ ,  $1 \times 10^{11}$ ,  $3 \times 10^{11}$ ,  $1 \times 10^{12}$ ,  $3 \times 10^{12}$  ions/cm<sup>2</sup>). The irradiated area of thin films was 1 cm<sup>2</sup>. SRIM 2008 [16] calculations show that

nuclear energy loss is  $9.640 \text{ eV/\AA}$ , which is negligible in comparison with electronic energy loss  $1.474 \times 10^3 \text{ eV/\AA}$ . Hence, SHI deposits energy to the material in form of electronic energy loss. Calculated stopping range of 100 MeV Ag ions in amorphous thin film samples is  $12.46 \mu\text{m}$ , which is greater than total thickness of the film (750 nm). Hence, Ag ions come to rest in the glass substrate after passing through the thin films. The thicknesses of the films were measured by the mechanical thickness profilometer (Tencore Instrument, Model Alpha Step 100). Amorphous natures of bulk samples and thin films were verified using X-ray diffraction measurements (Thermo Electron Corporation, Model ARL X'TRA) with  $\text{Cu K}\alpha$  radiation, and a scan rate of  $3^\circ/\text{minute}$ . EDAX measurements were performed to verify compositions of bulk sample, and thin films using an EDX detector attached with scanning electron microscope (SUPRA 40VP Carl Zeiss NTS GmbH). The optical transmissions for normal incidence of thin films were measured using a double beam UV/VIS computerized spectrophotometer (Hitachi, Model U-3300) in wavelength range of 300-900 nm. For structural analysis, micro-Raman measurements were performed on a spectrometer (Renishaw In Via Raman Microscope) using a 515.4 nm Argon ion laser with power density  $5 \text{ mW/cm}^2$  at room temperature at IUAC New Delhi.

### 3. Results and discussion

#### 3.1 XRD and EDAX Analysis:

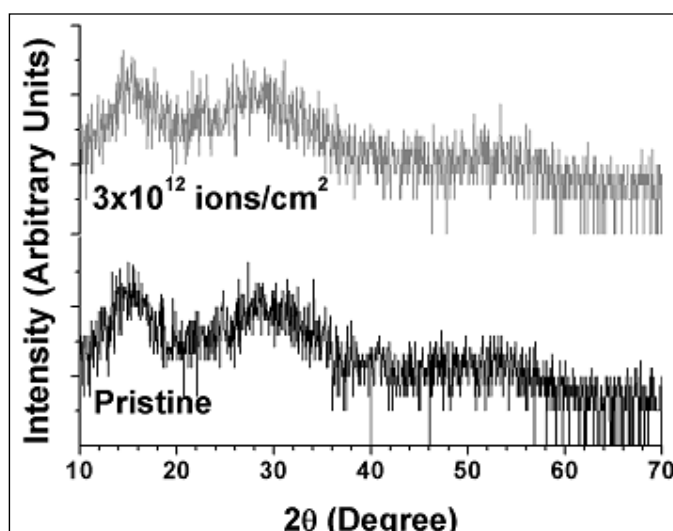


Fig. 1: XRD patterns

XRD patterns of pristine and irradiated thin film (fluence  $3 \times 10^{12} \text{ ions/cm}^2$ ) are shown in Fig. 1. Absence of sharp peak implies that thin films retain amorphous nature under swift-heavy ion irradiation. Presence of humps is verification of small to medium range order in amorphous thin films. Change in position of humps due to irradiation is an indication of changes in local structural arrangement, which is further explained using Raman measurements.

Fig. 2 shows EDAX measurements at different spots along with diameter in thin films, which predicts that chemical composition of amorphous thin films is  $\text{Ge}_{7.533}\text{As}_{38.698}\text{Se}_{53.769}$ . It is observed that thin film compositions show over stoichiometry in Se content, while deficient in Ge and As content than bulk sample, which is  $\text{Ge}_{10}\text{As}_{40}\text{Se}_{50}$ . The difference in stoichiometry of thin films and bulk sample is due to high melting points of As ( $817^\circ\text{C}$ ) and Ge ( $937^\circ\text{C}$ ) than Se ( $217^\circ\text{C}$ ).

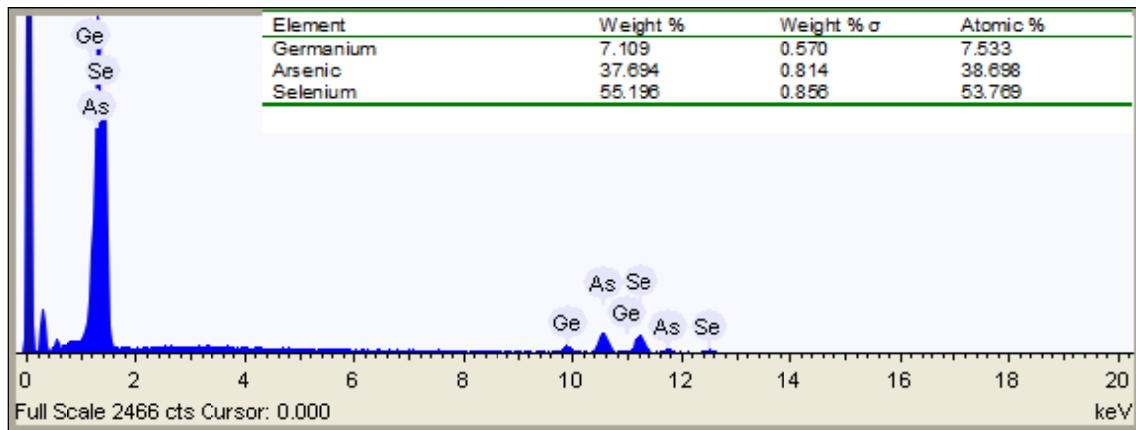


Fig. 2: EDAX spectrum of pristine thin film

### 3.2 Optical Transmission Analysis:

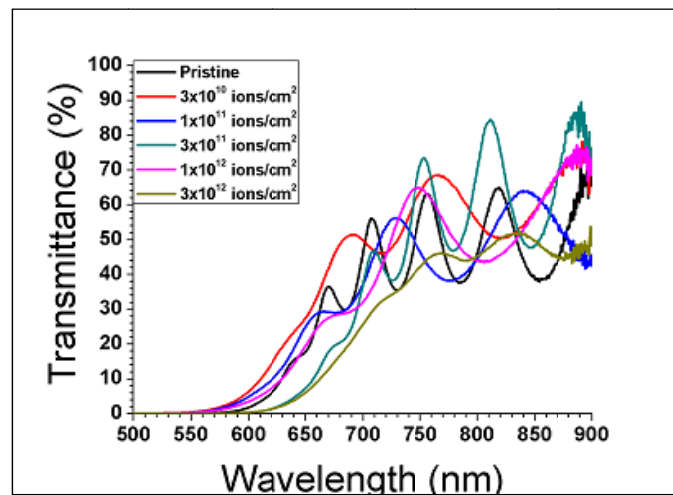


Fig. 3: Optical transmission spectra of pristine and irradiated thin films.

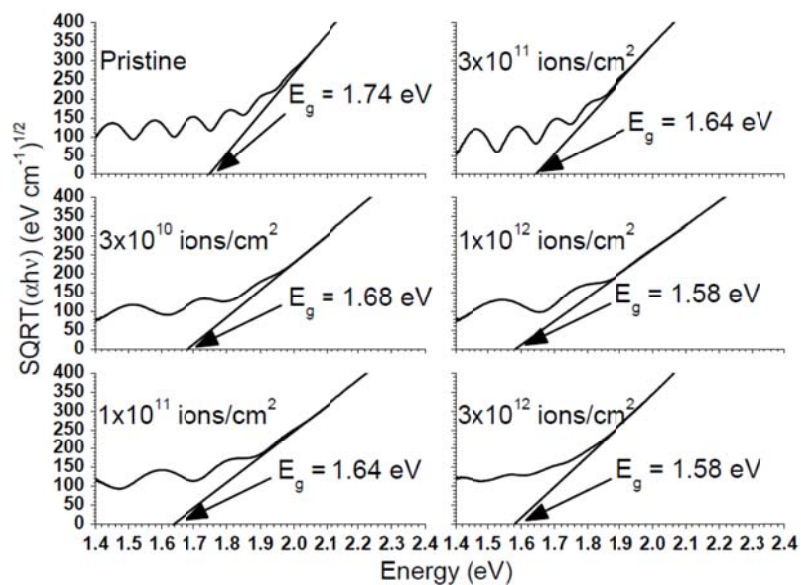


Fig. 4: Tauc's plot for pristine and irradiated thin films.

Fig. 3 shows the optical transmission spectra of pristine and irradiated amorphous  $Ge_{7.533}As_{38.698}Se_{53.769}$  thin films. The optical transparency of the films lies between 30 to 80 %. The transmission spectra contain interferences fringes in the wavelength range of  $\sim 650-900$  nm (visible range). Absorption coefficients ( $\alpha$ ) of pristine and irradiated thin films are determined from optical transmission spectra using the relation [17, 18]:

$$\alpha = (1/d) \ln(1/T) \quad (1)$$

where,  $d$  is film thickness and  $T$  is defined as the optical transparency of the films. The calculated values of  $\alpha$  at 710 nm are listed in Table 1, which increase from  $7944 \text{ cm}^{-1}$  to  $16004 \text{ cm}^{-1}$  with SHI irradiation increased up to fluence  $3 \times 10^{12} \text{ ions/cm}^2$ . The indirect optical bandgap ( $E_g$ ) is obtained from extrapolation of Tauc's plot [19], which is given as:

$$(\alpha h\nu)^{1/2} = B^{1/2}(h\nu - E_g) \quad (2)$$

where,  $B^{1/2}$  is coefficient and it is a measurement of disorder ( $B^{1/2} \propto 1/\text{width of localized states}$ , for  $\alpha \geq 10^4 \text{ cm}^{-1}$ ). From the value of  $B^{1/2}$  (as shown in the Table 1), it is clear that the disorders for irradiated  $Ge_{7.533}As_{38.698}Se_{53.769}$  thin films are higher than the pristine.

Obtained value of optical bandgap for pristine sample is 1.74 eV, which matches with the reported value of  $E_g$  (1.7-1.8 eV) for *Ge-As-Se* glasses at MCN $\sim 2.54$  [13, 20]. The optical bandgap decreases from 1.74 to 1.58 eV upon increase in fluence of SHI irradiation up to  $3 \times 10^{12} \text{ ions/cm}^2$ , as shown in Table 1. Reduction in optical bandgap can be understood in terms of Davis-Mott model [21], according to which, reduction in  $E_g$  is a consequence of increase in disorder under swift-heavy ion irradiation. Swift heavy ion irradiation increase local structural disorder, which is supported by Raman measurement (discussed in the section 3.3). Increase in local structural disorder cause increase in width of localized states, which reduces Tauc's parameter  $B^{1/2}$  as shown in Table 1.

Determination of linear refractive index ( $n_0$ ) is done using the relation [22, 23]:

$$[(n_0^2 - 1)/(n_0^2 + 2)] = 1 - (E_g/20)^{1/2} \quad (3)$$

Obtained value of  $n_0$  for pristine sample is 2.858, which lies within the range of *Ge-As-Se* glasses for MCN $\sim 2.54$  [13, 20]. Table 1 indicates that SHI irradiations increase the value of  $n_0$  from 2.858 to 2.945 up to fluence  $3 \times 10^{12} \text{ ions/cm}^2$ , which is a consequence of increase in disorder caused by SHI irradiation.

Determination of nonlinear refractive index can be done according to semi-empirical relation of Tichy *et al.* [24], which is:

$$n_2 \sim B^* / E_g^4 \quad (4)$$

where,  $B^* = 1.26 \times 10^{-9} [\text{esu} (\text{eV})^4]$ . Putting the value of  $E_g$ , we obtain  $n_2$  for pristine and irradiated thin films as shown in Table 1, which predicts that nonlinear refractive index lies within the range of *Ge-As-Se* glasses for MCN $\sim 2.54$  [20]. It increases from  $1.37 \times 10^{-10} [\text{esu}]$  to  $2.02 \times 10^{-10} [\text{esu}]$  upon swift-heavy ion irradiation up to fluence  $3 \times 10^{12} \text{ ions/cm}^2$ . The increase in nonlinear refractive index is a consequence of increase in disorder caused by SHI irradiation.

Table 1: Optical constants of pristine and irradiated thin films

Thin Film	$\alpha$ (at 710 nm) ( $\text{cm}^{-1}$ )	$E_g$ (eV)	$B^{1/2}$ ( $\text{cm eV}^{-1/2}$ )	$n_0$	$n_2$ [ $10^{-10}$ esu]
Pristine	7944.78	1.74	1052.63	2.858	1.37
$3 \times 10^{10}$ ions/ $\text{cm}^2$	10146.60	1.68	713.63	2.889	1.58
$1 \times 10^{11}$ ions/ $\text{cm}^2$	10419.67	1.64	674.74	2.911	1.74
$3 \times 10^{11}$ ions/ $\text{cm}^2$	10175.60	1.64	954.96	2.911	1.74
$1 \times 10^{12}$ ions/ $\text{cm}^2$	13152.45	1.58	624.24	2.945	2.02
$3 \times 10^{12}$ ions/ $\text{cm}^2$	16004.87	1.58	810.75	2.945	2.02

### 3.3 Raman Analysis

Figure 5 shows Raman plots for pristine and irradiated ( $3 \times 10^{12}$  ions/ $\text{cm}^2$ ) thin films. Analysis of Raman measurements is done using spectroscopic features available in Origin 8.0. An apparent view of Raman plots shows no major changes upon swift-heavy ion irradiations.

Raman plot of pristine thin films exhibits four peaks centred on  $192 \text{ cm}^{-1}$  (Peak 1),  $217 \text{ cm}^{-1}$  (Peak 2),  $240 \text{ cm}^{-1}$  (Peak 3),  $279 \text{ cm}^{-1}$  (Peak 4). Peak 1 is assigned as  $A_1$  mode, which is  $\nu_1$  symmetric stretching vibration mode of  $GeSe_{4/2}$  corner-sharing tetrahedral [26-31]. Origin of Peak 2 is not clear, which is identified as  $A_1^c$  companion peak due to either vibrations of  $Se$  atoms in four member rings composed of two edge-sharing tetrahedral [29-32], or stretching mode of  $Se-Se$  pairs [32]. Band 3 is the main band of  $As-Se$  glasses, which has the contribution of  $AsSe_{3/2}$  pyramidal units [28, 33] and  $Se-Se$  bonds in ring like or chain like structures [34]. Peak 4 ( $279 \text{ cm}^{-1}$ ) is assigned as the  $\nu_3$  stretching vibration mode of  $GeSe_{4/2}$  tetrahedral [27, 28].

Raman plot of thin film irradiated with fluence  $3 \times 10^{12}$  ions/ $\text{cm}^2$  exhibits five peaks at peak positions  $192 \text{ cm}^{-1}$  (Peak 1),  $214 \text{ cm}^{-1}$  (Peak 2),  $222 \text{ cm}^{-1}$  (New Peak),  $247 \text{ cm}^{-1}$  (Peak 3) and  $301 \text{ cm}^{-1}$  (Peak 4). It is clear from these plots that swift-heavy ion irradiation causes no changes in peak position of first peak ( $192 \text{ cm}^{-1}$ ). A shift towards lower wavenumber is observed for second peak ( $217$  to  $214 \text{ cm}^{-1}$ ), whereas shifts towards higher wavenumbers are observed for third peak ( $240$  to  $247 \text{ cm}^{-1}$ ) and fourth peak ( $279$  to  $301 \text{ cm}^{-1}$ ). In addition to that, a new peak is observed at peak position  $222 \text{ cm}^{-1}$ , which is assigned as vibration mode of  $As-As$  bonds [35, 36].

It is clear from Relative Area values in Table 2 and the above description that swift-heavy ion irradiation destructs stoichiometric units  $AsSe_{3/2}$  into wrong bonds ( $As-As$  bond and  $Se-Se$  bond), which increases disorder of the system. It is also clear from Table 2 that relative area corresponding to Peak 1 is approximate 13% and it remains almost constant upon swift-heavy ion irradiation. This indicates that number of  $GeSe_{4/2}$  CST units remain almost unchanged, while number of  $AsSe_{3/2}$  pyramidal units reduces upon swift-heavy ion irradiation. The  $GeSe_{4/2}$  corner-sharing tetrahedral are three dimensional and more compact structural units than layered  $AsSe_{3/2}$  triangular units, hence, SHI irradiation distracts  $AsSe_{3/2}$  pyramidal units, whereas,  $GeSe_{4/2}$  corner sharing units remain unchanged upon SHI irradiation. In addition to that,  $GeSe_{4/2}$  tetrahedral units are constructed with stronger  $Ge-Se$  bonds (bond energy =  $49.42 \text{ kcal/mol}$ ), while  $As-Se$  bonds (bond energy =  $41.69 \text{ kcal/mol}$ ) are building block of  $AsSe_{3/2}$  units. Hence, swift-heavy ion irradiation breaks comparatively weaker bonds ( $As-Se$ ) in comparison of stronger bonds ( $Ge-Se$ ). It is also observed from Table 2 that FWHM corresponding to Peak 1 ( $GeSe_{4/2}$  CST) increases from  $15.25$  to  $16.29$  upon swift-heavy ion irradiation, which also justifies that swift-heavy ion irradiation increases local structural disorder in amorphous  $Ge_{7.533}As_{38.698}Se_{53.769}$  thin film.

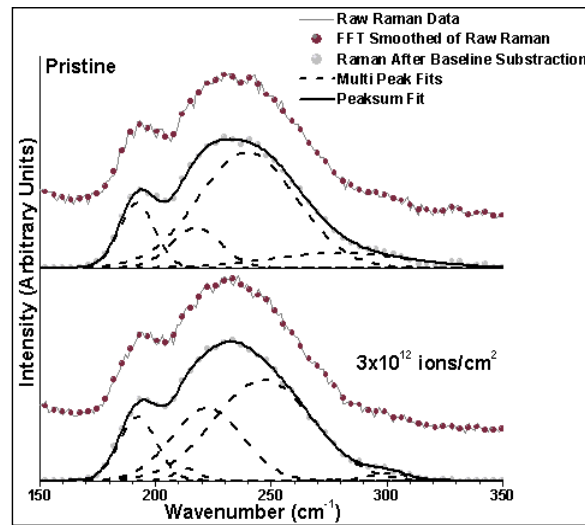


Fig. 5: Raman plots of pristine and irradiated thin films.

Another important behaviour noticed upon swift-heavy ion irradiation is in optical elasticity, which is proportional to square of the mode frequency of corner-sharing tetrahedral ( $\nu_{CS}^2$ ) [37]. It increases systematically as network connectivity increases upon cross-linking. In IP phase and stressed-rigid phase,  $\nu_{CS}^2$  is proportional to optical elasticity, which is called elasticity power law [37]. The above findings becomes more important as optical elasticity, in case of swift-heavy ion irradiation, is maintained up to the fluence  $3 \times 10^{12}$  ions/cm<sup>2</sup> (it can be easily determined as no change is observed in the position of first peak), which is a threshold limit of ion exposure in our study. Further, increase in fluence causes thermal destruction at the surface of the film. This behaviour, as shown by amorphous chalcogenide composition in the present study, is not the default behaviour of IP phase and stressed rigid phase compositions during photoexposure of high power density (factor of  $10^3$ ). High power density photoexposure causes a collapse in IP phase (cooperatively self-organized network structure) to form a random network structure [38], whereas, present study indicates that ion irradiation is not causing a change in optical elasticity up to the destruction limit. This exploitation found in the present study is important for the optical applications, which require optical changes using treatment techniques (photo/ion), while optical elasticity of the material needs to be maintained.

Table 2: Raman peak details of pristine and irradiated ( $3 \times 10^{12}$  ion/cm<sup>2</sup>) thin films.

Peak Details	Pristine			Irradiated ( $3 \times 10^{12}$ ions/cm <sup>2</sup> )		
	Peak Position (cm <sup>-1</sup> )	Width	Relative Area	Peak Position (cm <sup>-1</sup> )	Width	Relative Area
<b>Peak 1:</b> A <sub>1</sub> bond stretching mode of GeSe <sub>4/2</sub> corner-sharing tetrahedral [26-31]	192	15.26	13	192	16.29	13
<b>Peak 2:</b> A <sub>1</sub> <sup>C</sup> companion mode of either edge-sharing tetrahedral GeSe <sub>4/2</sub> or stretching mode of Se-Se pairs[29-32]	217	21.40	11	214	10.75	2
<b>Peak 3:</b> Main Band of As-Se glasses due to AsSe <sub>3/2</sub> pyramidal units and Se-Se bonds [28,33,34]	240	42.47	65	247	42.68	55
<b>Peak 4:</b> $\nu_3$ stretching vibration of GeSe <sub>4/2</sub> [27,28]	279	58.21	11	301	17.17	2
<b>New Peak:</b> Vibration mode of As-As bonds [35,36]				222	30.64	28

#### 4. Conclusion

Swift-heavy ion (100 MeV Ag ions) irradiation causes reduction in optical bandgap ( $E_g$ ), while increase in linear refractive index ( $n_0$ ) and nonlinear refractive index ( $n_2$ ) till fluence  $3 \times 10^{12}$  ions/cm<sup>2</sup> in the intermediate-phase amorphous composition Ge<sub>7.533</sub>As<sub>38.698</sub>Se<sub>53.769</sub> thin films. These changes are the consequence of increase in disorder, which is supported by Raman measurements.

In addition, stability in GeSe<sub>4/2</sub> CST units indicates that optical elasticity remains almost unchanged upon 100 MeV Ag swift-heavy ion irradiation up to fluence  $3 \times 10^{12}$  ions/cm<sup>2</sup>, while optical nonlinearity is increased.

The present study is helpful in understanding the threshold limits and tuning of optical/structural properties of amorphous Ge-As-Se intermediate phase compositions under ion irradiations. The present study can be extended to update the fabrication protocols using ion irradiations upon network glasses for threshold conditions to produce optical components with improved performance.

#### Acknowledgement

The author as the Principal Investigator of Minor Research Project: F. No. 8-3 99/2011 (MRP/NRCB) is thankful to UGC for providing funds for this work. The author is also thankful to IUAC for providing Beam time and other experimental facilities required for this work as BTR No & Activity: 49102 MS. Dr. D. K. Avasthi, (Scientist-H, and IUAC collaborator in this project) had a major role in the successful measurements required within IUAC. Useful inputs are provided by Dr. Ambuj Tripathi, Dr. Fouren Singh and other IUAC personnel and author is willing to thank them all.

#### References

- [1] A. Zakery and S. R. Elliot, *J. Non-Cryst. Solids*. **330**, 1 (2003).
- [2] B. J. Eggleton, B. Luther-Davies and K. Richardson, *Nature Photon*. **5**, 141 (2011).
- [3] *Photo-Induced Metastability in Amorphous Semiconductors*, edited by A. V. Kolobov, Wiley-VCH, Weinheim (2003).
- [4] D. K. Avasthi and G. K. Mehta, *Swift Heavy Ions for Materials Engineering and Nanostructuring*, SprinSr, Netherlands (2011).
- [5] F. Qiu, T. Narusawa, and J. Zheng, *Appl. Opt.* **50**, 733 (2011).
- [6] D. Freeman, S. Madden, B. Luther-Davies, *Opt. Exp.* **13**, 3079 (2005).
- [7] Z. U. Borisova, *Glassy Semiconductors*, Plenum Press, Newyork (1981).
- [8] J. T. Gopinath, M. Sojagic, E. P. Ippen, V. N. Fuflyingin, W. A. King, M. Shurgailn, *J. Appl. Phys.* **96**, 6931 (2004).
- [9] J. C. Phillips, *J. Non-cryst. Sol.* **34**, 153 (1979).
- [10] M. F. Thorpe, D. J. Jacobs, and B. R. Djordjevic, *The structure and rigidity of network glasses, in insulating and semiconducting glasses*, Ed. P. Boolchand, pp 94, Worldscientific (2000).
- [11] K. Tanaka, *Phys. Rev. B* **39**, 1270 (1989).
- [12] P. Boolchand, D. G. Georgiev, B. Goodman, *J. Opt. Adv. Mat.* **3**, 703 (2001).
- [13] D. A. P. Bulla, R. P. Wang, A. Prasad, A. V. Rode, S. J. Madden, B. Luther-Davies, *Appl. Phys. A* **96**, 615 (2009).
- [14] A. Prasad, C.J. Zha, R. P. Wang, A. Smith, S. Madden and B. Luther-Davies, *Opt. Express*. **16(4)**, 2804 (2008).
- [15] G. Yang, H. Jain, A. Ganjoo, D. Zhao, Y. Xu, H. Zeng and G. Chen, *Opt Express* **16[14]**, 10565 (2008).
- [16] J. F. Ziegler, SRIM-2008, v. 2008.03. Available from <http://www.srim.org>.
- [17] R. Chauhan, A. K. Srivastava, M. Mishra, K. K. Srivastava, *Integr. Ferroelectr.* **119**, 22 (2010).

- [18] A. K. Srivastava, S. Thota, and J. Kumar, *J. Nanosci. and Nanotechnol.* **8**, 4111 (2008).
- [19] J. Tauc, *Amorphous and Liquid Semiconductors*, Plenum Press, Newyork, 1979.
- [20] B. Luther-Davies, Z. Congji, A. Prasad and A. Smith in *Conference on Lasers and Electro-Optics/Quantum Electronics and Laser Science Conference and Photonic Applications Systems Technologies*, OSA Technical Digest Series (CD), paper CMGG7, Optical Society of America (2007).
- [21] N. F. Mott and E. A. Davis, *Electronic Processes in Non-Crystalline Materials*, 2nd Edition, Clarendon, Oxford, pp. 497 (1979).
- [22] V. Dimitrov, S. Sakka, *J. Appl. Phys.* **79**, 1741 (1996).
- [23] A. K. Srivastava, J. Kumar, *AIP Advances* **1(3)**, 032153(1) (2011).
- [24] H. Tichá, L. Tichý, *J. Optoelectron. Adv. M.* **4[2]** 381 (2002).
- [25] R. Chauhan, A. K. Srivastava, A. Tripathi, K. K. Srivastava, *PNS-MI.* **21**, 205 (2011).
- [26] T. Usuki, O. Uemura, K. Fujimura, Y. Kameda, *J. Non-Cryst. Solids* **192**, 69 (1995).
- [27] G. J. Ball, J. M. Chamberlain, *J. Non-Cryst. Solids* **29**, 239 (1978).
- [28] V. Q. Nguyen, J. S. Sanghera, J. A. Freitas, I. D. Aggarwal, I. K. Lloyd, *J. Non-Cryst. Sol.*, **248**, 103 (1999).
- [29] S. Sugai, *Phys. Rev. B* **35**, 1345 (1987).
- [30] A. Kumar, S. K. Tripathi, P. K. Kulriya, A. Tripathi, F. Singh, D. K. Avasthi, *J. Phys. D: Appl. Phys.* **43**, 1 (2010).
- [31] P. K. Dwivedi, S. K. Tripathi, A. Pradhan, V. N. Kulkarni, S. C. Agarwal, *J. Non-Cryst. Solids* **266-269**, 924 (2000).
- [32] G. Petrash, *Optica I Spectroskopia (in Russian)* **9**, 423 (1960).
- [33] K. Saitoh, O. Uemura, T. Usuki, Y. Kameda, *J. Non-Cryst. Solids* **192&193**, 286 (1995).
- [34] G. Lucovsky in *Gelash, P. Grosse (Eds), The Physics of Selenium Tellurium*, Springer, Berlin, pp. 120 (1979).
- [35] M. Frumar, Z. Polak, Z. Cerosek, *J. Non-Cryst. Solids* **256-257**, 105 (1999).
- [36] R. Ston, M. Vlcek, H. Jain, *J. Non-Cryst. Solids* **326-327**, 220 (2003).
- [37] P. Boolchand, X. Feng, W. J. Bresser, *Journal of Non-Crystalline Solids* **293**, 348 (2001).
- [38] F. Fritzsche, edited by P. Boolchand, *World Scientific Publishing Co Pte Ltd, Singapore* (2000).